Pharmaceutical Research, Vol. 25, No. 3, March 2008 (© 2007)
DOI: 10.1007/s11095-007-9389-y

Research Paper

Targeted Delivery of Complexes of Biotin–PEG–Polyethylenimine and NF-κB Decoys to Brain-derived Endothelial Cells *in Vitro*

Raktima Bhattacharya,[1] Berit Osburg,[1] Dagmar Fischer,[1,2] and Ulrich Bickel[1,3]

Received May 3, 2007; accepted June 22, 2007; published online October 20, 2007

Purpose. To evaluate the effect of re-directing the uptake mechanism of polyplexes containing oligodeoxynucleotide (ODN) decoys to nuclear factor kappa B (NF-κB) from absorptive-mediated to receptor-mediated endocytosis.
Materials and Methods. Complexes of ODNs and a co-polymer of biotin–polyethylenglycol and polyethylenimine (BPP) were targeted to brain-derived endothelial cells with a conjugate of antibody 8D3 and streptavidin (8D3SA). Size and stability of ODN/BPP complexes was measured by dynamic light scattering. Cellular uptake was studied by confocal microscopy. Cell viability and pharmacological effects were investigated on murine bEnd5 cells stimulated with tumor necrosis factor.
Results. ODN/BPP complexes showed sizes of 116±2.3 nm, which increased by 40 nm when coupled to 8D3SA, and were stable in physiological fluids. Targeted complexes were internalized intact into endosomal compartments. Treatment conditions, which yielded significant inhibitory effects on mRNA expression of VCAM-1, ICAM-1, IκBα and iNOS by bEnd5 cells, did not affect viability. At 0.5 μM, decoy ODN significantly inhibited monocyte adhesion to bEnd5 monolayers when delivered as 8D3SA-targeted complex, while higher concentrations of untargeted complex were ineffective.
Conclusions. The complex of NF-κB decoys and BPP, which can be targeted to transferrin receptors, is a promising drug candidate for neuroinflammatory diseases affecting the blood–brain barrier.

KEY WORDS: blood–brain barrier; drug delivery; polyethylenimine; transferrin receptor; transcription factor decoy.

INTRODUCTION

The potential of transcription factor decoys, short double stranded oligonucleotides (ODNs), as novel drugs has received increasing attention (1). Decoys for various transcription factors, e.g. nuclear factor kappaB (NF-κB), may thus expand the range of oligonucleotide-based gene therapeutics, which comprises classes like antisense drugs, ribozymes, and siRNAs. The prime obstacle to conquer before clinically useful drugs based on all of these classes of agents will become reality is delivery and targeting to the site of action. Recently, we demonstrated efficient transfection of endothelial cells with decoy ODNs after complexation with polyethylenimines (2). That report also showed that the intracellular delivery results in anti-inflammatory pharmacological effects, as indicated by inhibition of VCAM-1 expression and of monocyte adhesion to the endothelial cells *in vitro*. The bEnd5 endothelial cells utilized in these studies are derived from brain microvessels, which form the anatomical substrate of the blood–brain barrier (BBB). The BBB not only restricts brain entry of solutes, but it also controls the trafficking of leukocytes. Because lymphocyte and monocyte extravasations across the BBB play a pivotal role in neuroinflammation, consequently the inhibition of adhesion molecules or their ligands is an attractive therapeutic strategy (3,4). Vascular cell adhesion molecule-1 (VCAM-1), expressed on the endothelial cells, and its ligand, α4β1-integrin, expressed on the leukocyte surface, are major players in this process (4). The viability of a strategy aimed at inhibition of adhesion molecules has recently been clinically proven in patients with MS by the high therapeutic efficacy of an α4-integrin monoclonal antibody, natalizumab (5).

The ODN/PEI polyplexes used in the previous study were non-targeted (2). Therefore, cellular uptake occurred by adsorptive-mediated endocytosis, which is triggered by electrostatic interactions between the negatively charged plasma membrane and the positively charged complexes. As

[1] Department of Pharmaceutical Sciences, Texas Tech University Health Sciences Center School of Pharmacy, 1300 Coulter Drive, Amarillo, Texas 79106, USA.
[2] Department of Pharmaceutics and Biopharmacy, Philipps-University of Marburg, Marburg, Germany.
[3] To whom correspondence should be addressed. (e-mail: Ulrich.Bickel@ttuhsc.edu)

ABBREVIATIONS: BBB, blood–brain barrier; BCECF-AM, 2′,7′-*bis*-(carboxyethyl)-5-(6)-carboxyfluorescein-acetoxymethyl ester; BPP, biotin–polyethylenglycol–polyethylenimine; ICAM-1, intercellular adhesion molecule 1; LMW-PEI, low molecular weight polyethylenimine; NF-κB, nuclear factor kappaB; ODN, oligodeoxynucleotide; PEG, poly (ethylene glycol); PEI, polyethylenimine; SA, streptavidin; S-SMPB, sulfosuccinimidyl 4-[*p*-maleimidophenyl]butyrate; VCAM-1, vascular cell adhesion molecule 1; 8D3SA, 8D3-streptavidin.

we found in pharmacokinetic experiments with such cationic complexes, they are subject to rapid clearance by liver, spleen and kidney after systemic administration (6). Therefore, efficient re-direction to the desired organ vascular bed is required for potential *in vivo* applications targeting organs other than those mentioned above, such as brain. On one hand, the microvasculature supplying brain tissue, due to its physiological barrier function, poses a special challenge to the delivery of macromolecular drugs and nanoparticles. On the other hand, BBB endothelial cells express several receptor-mediated uptake mechanisms, including the transferrin receptor system, which can be utilized for targeted drug delivery (7,8). In the current study ODN/PEI complexes were targeted to the transferrin receptor, using a conjugate of the rat anti mouse antibody 8D3 (9) and streptavidin (designated 8D3SA). 8D3 has been used successfully as vector for brain delivery of peptides, proteins, peptide nucleic acids and plasmids (10–13). For ODN complex formation, we utilized the same PEI of low molecular weight (PEI 2.7 kDa), which gave the best response with the nontargeted polyplexes (2), has low cytotoxicity, and also possesses high transfection efficiency for plasmid DNA (14). This low molecular weight PEI was PEGylated with polyethylenglycol (3.4 kDa) carrying a terminal biotin moiety. Complexes between NF-κB decoy ODN and biotinylated PEG-PEI (designated BPP) could therefore be conveniently coupled to the 8D3SA vector via streptavidin/biotin linkage.

MATERIALS AND METHODS

Cell Culture

The bEnd5 endothelial cell line (a kind gift from Dr. Britta Engelhardt, Bern, Switzerland) is derived from mouse brain and was generated by immortalization with polyoma middle T oncogene (15). Cells were grown in DMEM (Mediatech Inc. Cellgro, Herndon, VA, USA) supplemented with 10% (v/v) FBS (fetal bovine serum) (Bio Whittacker, Walkersville, MD, USA), 1 mM sodium pyruvate, 4 mM L-glutamine, 1% (v/v) non-essential amino acids, 1% (v/v) 10,000 IU/ml penicillin 10,000 μg/ml streptomycin (all Mediatech Inc. Cellgro), 0.0004% β-mercaptoethanol (Sigma, St. Louis, MO, USA). The human monocytic leukemic cell line U-937 (ATCC, Manassas, USA) was cultured in RPMI1640 (Mediatech Inc., Cellgro) using the same media supplements as the bEnd5 cells. Both cell lines were maintained at 37°C, 5% CO_2 and 95% relative humidity.

8D3 Production and Conjugation with Streptavidin

The 8D3 hybridoma (rat-anti-mouse transferrin receptor, IgG_{2a}) was obtained from Dr. Britta Engelhardt (Bern, Switzerland) and antibody was produced by ascites generation in nude mice (QED, San Diego, CA, USA). IgG purification from ascites fluid was accomplished by affinity chromatography on Protein-G HiTrap columns (Amersham Biosciences, Piscataway, NJ, USA).

A conjugate of 8D3 and streptavidin (SA) was synthesized as follows: 5 mg purified 8D3 antibody was thiolated using 33.3 μl Traut's reagent (1.38 mg/ml in DMSO) (Pierce Biotechnology, Rockford, IL, USA) under gentle mixing for 60 min at room temperature. Then 1.875 mg recombinant streptavidin (Sigma, St. Louis, MO, USA) was activated using 15 μl of 4.58 mg/ml sulfosuccinimidyl 4-[*p*-maleimidophenyl]-butyrate (S-SMPB, Pierce Biotechnology) in dimethylformamide. Both reactions were quenched by adding a molar excess of glycine for 30 min at room temperature. Thiolated 8D3 and MBP-streptavidin were purified from the reaction mixtures on PD-10 columns (Amersham Biosciences) eluted with 20 mM PBS / 1 mM EDTA pH 7.0, and 0.5 ml eluate fractions were collected. Protein concentration in the fractions was estimated by the Coomassie Blue reagent method following the manufacturer's protocol (Pierce Biotechnology). The protein peak fractions of thiolated 8D3 and MBP-streptavidin were combined (final volume 2–3 ml) and the conjugation reaction was allowed to proceed on ice for 2 h under gentle stirring. The reaction was quenched by addition of iodoacetamide (Sigma) and a trace amount of 0.5 μCi [^{3}H]biotin (Amersham Biosciences, NJ, USA) was added before chromatographic purification by FPLC over Superdex 200 HR 10/30. Aliquots from 1 ml eluate fractions were counted for ^{3}H activity in a Beckman 6000 scintillation counter (Beckman, Fullerton, CA, USA) and overlaid with the UV absorption trace. Fractions corresponding to a 1:1 conjugate of 8D3 and SA were pooled and concentrated. The protein concentration was determined by the BCA method (Pierce Biotechnology) and the 8D3SA conjugate was stored at −20°C.

Preparation of ODN/Polyethylenimine Complex

The low molecular weight PEI (LMW-PEI) used here was synthesized by acid catalyzed ring opening polymerization of aziridine in aqueous solution (16), which results in a low branched PEI (ratio of primary/secondary/tertiary amines=1:2:1) with a molecular weight of 2.7 kDa. For synthesis of biotinylated PEGylated PEI (designated BPP), LMW-PEI and Poly(ethylene glycol)-α-biotin-ω-NHS ester (molecular weight 3.7 kDa; Shearwater, Huntsville, AL, USA) were reacted in $CHCl_3$ at equimolar concentration for 18 h under boiling (17). Completeness of the reaction and the 1:1 molar composition of the final BPP product were confirmed by ^{1}H-NMR.

The ODN used in these experiments was a double-stranded 20mer phosphodiester ODN synthesized from the complementary single-stranded ODNs (MWG-Biotech, Highpoint, NC, USA) by heating to 95°C for 5 min, followed by stepwise decrease to ambient temperature (2). The sequence of the decoy ODN (NF-κB decoy), with consensus sequence underlined, is:

5′-CCT TGA AGG GAT TTC CCT CC-3′
3′-GGA ACT TCC CTA AAG GGA GG-5′

A scrambled dsODN with the following sequence

5′-TTG CCG TAC CTG ACT TAG CC-3′
3′-AAC GGC ATG GAC TGA ATC GG-3′

or salmon sperm DNA (Brinkmann-Eppendorf, Westbury, NY, USA) were used as negative controls. Complexes were prepared by mixing ODN and BPP in 10 mM Na-phosphate/0.9% NaCl (PBS) and incubating for 10 min at room temperature. The ratio of ODN and BPP was 6:1 based on N/P ratio [polymer nitrogen (N) per DNA phosphate (P)]. Pilot experiments had shown that all the ODN was bound in

complexes formed at N/P ratios above 3:1, but maximal condensation was seen at N/P=6:1, as detected by dye-exclusion of ethidium bromide on 1% agarose gel electrophoresis. Complexes for targeting to transferrin receptors were obtained by adding 8D3SA in PBS to the ODN/PEI complex and further incubation for 15 min.

Particle Characterization

Complex size, either of ODN/BPP or 8D3SA-ODN/BPP, in PBS solutions was investigated by photon correlation spectroscopy using a submicron particle sizer Nicomp 380/ZLS equipped with a 15 mW Laser diode with a wavelength of 635 nm (Particle Sizing Systems, St. Barbara, CA, USA). Complex sizes were measured after 10 min, 1 h, 4 h, 8 h, 24 h and 1 week using intensity weighted Gaussian fitting. For determination of zeta potential, ODN/BPP complexes were made in 5% Glucose/10 mM HEPES, pH 7.4 and after 10 min were measured in the Nicomp 380/ZLS using the zeta potential module (E-field 1V/cm, phase shift analysis with software ZPW 388, version 1.70).

Cytotoxicity

In vitro cytotoxicity of the complex on bEnd5 cells was measured as described (2) using the EZ4U kit (Alpco Diagnostics, Windham, NY, USA) and following the manufacturer's instructions. This assay is a modified version of the 3-(4,5-Dimethylthiazol-2-yl)-2,5-diphenyltetrazolium bromide (MTT) assay. Mitochondrial metabolism generates a water-soluble formazan derivative not requiring an additional solubilization step. Briefly, bEnd5 cells were grown to confluence in 96-well plates and were exposed to the complexes in culture media over a time period of 8 h, followed by 4 h of TNFα treatment (corresponding to the pharmacologic experiments described below). The media was changed after TNFα stimulation, 20 μl per well of substrate solution were added, and plates were incubated for another 2 h at 37°C. The absorbance of the reaction product was measured at 492 nm (with reference wavelength 560 nm) in an ELISA plate reader. Viability data were normalized by wells with naïve cells, i.e. treated neither with complex nor TNFα. The mean absorption value of these wells was set to 100%.

Endothelial Cell Treatment

Cells were grown to confluency on 6-well plates (for real time PCR) or 24-well plates (for adhesion experiments). Triplicate wells were treated for 8 h with DNA/BPP complexes at 0, 0.5, 1.0, or 2.0 μM concentrations of decoy ODN, or 10 μg/ml salmon sperm DNA, or 2.0 μM scrambled ODN. The N/P ratio of the complexes was always 6:1, and they were added either with the delivery vector 8D3SA (at 0.75 μM final concentration) or without it. Media was used in presence of 10% fetal bovine serum (FBS), or serum-free. After 8 h, media was exchanged to new media with 50 ng/ml TNFα (Pepro Tech, Rocky Hill, NJ, USA) to stimulate the cells for 4 h. The cells stimulated with TNFα only, but not treated with complex, are referred to as "media control". In separate series of experiments, concentrations of ODN or 8D3SA were varied.

Confocal Microscopy

bEnd5 cells were grown on coverslips and incubated in culture media with fluorescent labeled ODN/BPP complex (0.5 μM ODN concentration), with or without 8D3SA, for 2 h at 37°C. The PEI in these complexes was labeled with NHS-rhodamine (Pierce, Rockford, IL, USA). Briefly, BPP (2 mg in 1 ml H2O, pH adjusted to 7.4 with HCl) was reacted with NHS-rhodamine (0.1 mg/100 μl DMSO) for 2 h on ice. Rhodamine-BPP was separated from non-reacted NHS-rhodamine by gel chromatography on PD-10 columns (GE Healthcare, Piscataway, NJ). The degree of substitution was calculated from the known molar quantities of BPP and NHS-rhodamine in the reaction mixture and the fluorescence peak areas corresponding to rhodamine-BPP and free rhodamine in the eluate, respectively. Recovery for both rhodamine-BPP and rhodamine from these columns was >90% as determined in separate chromatographic runs. Twenty-nine percent of BPP molecules carried a rhodamine conjugate, on average. Rhodamine-BPP was mixed with custom synthesized 5′-FITC-ODN (MWG-Biotech, High-point, NC, USA).Nuclear staining was performed with DRAQ5 (Biostatus Ltd., Leicestershire, UK) following manufacturer's protocol. The cells were fixed with 4% paraformaldehyde and washed with wash buffer thrice and once with water. The coverslips were placed on slides with glycerol as mounting media (Mallinckrodt, St. Louis, MO, USA) and sealed with Histoseal (Bioworld, OH, USA). The samples were viewed under a Leica IRE2 microscope equipped with the TCS-SL spectral confocal scanner (Leica Microsystems, Heidelberg, Germany). Excitation wavelengths were 488 nm (Argon laser), 543 nm (HeNe) and 633 nm (GreNe) for excitation of FITC, Rhodamine and DRAQ5, respectively.

RNA Extraction and Reverse Transcription

RNA was extracted from bEnd5 cells plated on 6-well plates using the TRIZOL Reagent (Invitrogen, Carlsbad, CA, USA) according to the manufacturer's instructions. Two micrograms of RNA from each sample was then reverse transcribed to cDNA by SuperscriptII Reverse Transcriptase (Invitrogen) using random hexamers. cDNA was diluted fourfold and stored at −20°C until further use.

Quantitative Real Time PCR

The mRNA expression of VCAM-1, truncated VCAM-1, ICAM-1, iNOS, IκBα was analyzed on an automated sequence detection system model 5700 (Applied Biosystems, Foster City, CA, USA) using fluorogenic probes. Quantification was performed using the following forward and reverse primers: VCAM-1: 5′-TGC AAA GGA CAC TGG AAA AGA G-3′; 5′-GCC CAC TCA TTT TAA TTA CTG GAT-3′; VCAM-1 truncated: 5′-TGT GTG AAG GAG TTA ATC TGA TTG-

3′; 5′-GGC CAT TAG TAA TCT GAG ACT TCA TTC-3′; ICAM-1: 5′-AGT CGT CCG CTT CCG CTA C-3′; 5′-CTG GCA GAG GTC TCA GCT CC-3′
iNOS: 5′-CAG CTG GGC TGT ACA AAC CTT-3′; 5′-CAT TGG AAG TGA AGC GTT TCG-3′
IκBα: 5′-CCA ACT ACA ATG GCC ACA CG-3′; 5′-GTG CTC CAC GAT GGC CAG-3′

The probes used were
VCAM-1: 5′-ACC CAG GTG GAG GTC TAC TCA TTC CCT GA-3′; VCAM-1 truncated (18): 5′-ACA AAG CAG AAG TGG AAT TAG TTG TTC AAG TGG G-3′; ICAM-1: 5′-TCA CCG TGT ATT CGT TTC CGG AGA GTG-3′
iNOS: 5′-CGG GCA GCC TGT GAG ACC TTT GA-3′
IκBα: 5′-TCT GCA CCT AGC CTC TAC TCA CGG CT-3′
with the 5′-nucleotide labeled with the fluorescent dye 6-FAM (6-carboxy fluorescein) and the 3′-nucleotide labeled with a quencher dye (TAMRA=6-carboxy-tetramethyl rhodamine) (MWG-Biotech). All other PCR reagents were obtained from Applied Biosystems. 18s rRNA detection kit (Applied Biosystems) was used as internal control. Reverse transcribed RNA from non-treated and TNFα stimulated cells (media control) served as negative and positive control, respectively. Control amplifications (no template) were included in each reaction. The reaction was carried out in optical 96-well plates (Applied Biosystems) with 2 μl sample (50 ng cDNA) added to 23 μl reaction mix containing 1× PCR Gold buffer, 5 mM $MgCl_2$, 200 μM dNTPs each, 300 nM forward and reverse primers each, 100 nM probe, 0.01 U/μl Amp Erase UNG, and 0.05 U/μl AmpliTaq Gold. PCR conditions were as follows: 2 min at 50°C for UNG incubation, 10 min at 95°C for the activation of AmpliTaq Gold DNA polymerase, and 40 cycles of 15 s at 95°C and 1 min at 60°C. All experiments were carried out in triplicates. The "delta-delta" method was used for evaluation, i.e. for each individual sample, the threshold cycle number of VCAM-1, ICAM-1, iNOS, IκBα and GAPDH was corrected by the threshold cycle number of 18S rRNA. Then, the 18S-corrected signal of the non-treated control sample (NT) was set to 1 and all other samples were expressed as fold-stimulation compared to NT.

Monocyte Adhesion Assay

Adhesion assays were performed as described previously (2). Briefly, confluent bEnd5 cells were treated with the ODN/BPP complexes in both serum free and serum conditions, incubated for 8 h and activated by TNFα for 4 h. Then 10^6 cells/well human monocytic leukemia U-937 cells (ATCC, Manassas, VA, USA) labeled with 1 μg/ml 2′,7′-*bis*-(carboxyethyl)-5-(6)-carboxyfluorescein-acetoxymethyl ester (BCECF-AM) were added to the bEnd5 cells and incubated for 30 min. Nonadherent cells were washed off and adherent cells were lysed to measure the fluorescence (F) at 492 nm (excitation) and 535 nm (emission). The monocyte adhesion was calculated as:

$$Adhesion[\%] = 100 \times F_{sample}/F_{total}$$

where F_{total}=fluorescence intensity of 10^6 cells.

Statistical Analysis

Statistical comparisons were carried out using GraphPad Prism (Mac version 4.0c) by single factor analysis of variance (ANOVA) of untransformed data or after log transformation. Dunnett's multiple comparisons post-test was applied.

RESULTS

Particle Characterization

Complex sizes of ODN/BPP (N/P ratio 6:1) with and without coupling of the targeting vector (8D3SA) are shown in Fig. 1. The average complex size of freshly prepared ODN/BPP was 116±2.4 nm (mean±SE, n=3) as determined by quasielastic light scattering. Size increased slightly to 138 nm over the first 8 h, with no further change detectable up to 7 d. Measurements in presence of 10% serum yielded sizes between 30 and 60 nm larger compared to complexes in PBS without serum. The difference was only seen at time points up to 8 h, at later time points the sizes were similar in samples with or without serum. Coupling of the targeting vector 8D3SA to ODN/BPP complexes resulted in a size increase of 30 to 40 nm. The zeta potential of ODN/BPP complexes (N/P ratio 6:1) in 5% glucose/ 10 mM HEPES at pH 7.4 was determined as 13.7±5.0 mV (mean±SE, n=4).

Effect of NF-κB Decoy ODN Treatment on Endothelial Cells

All *in vitro* experiments aimed at demonstration of potential cytotoxicity, cellular uptake, and pharmacologic effects of ODN/BPP complexes on pro-inflammatory responses were performed on bEnd5 cells, a mouse brain-derived endothelial cell line (19).

Cytotoxicity

The *in vitro* cytotoxicity of BPP was tested at different concentrations of NF-κB decoy ODN, scrambled ODN and salmon sperm DNA, all at 6:1 N/P ratio. The potential

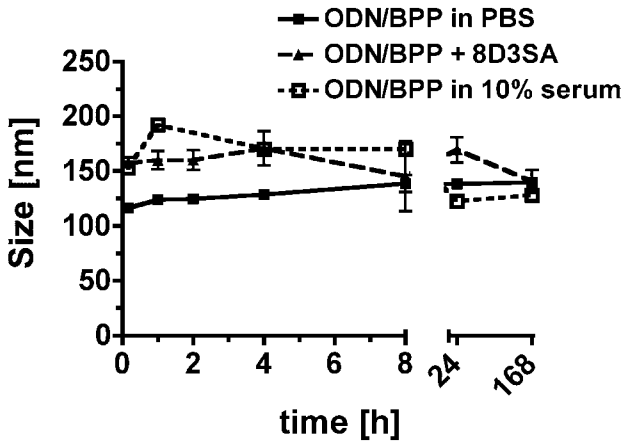

Fig. 1. Size and stability as measured by photon correlation spectroscopy. Measurements were performed in triplicate and expressed as mean±SD.

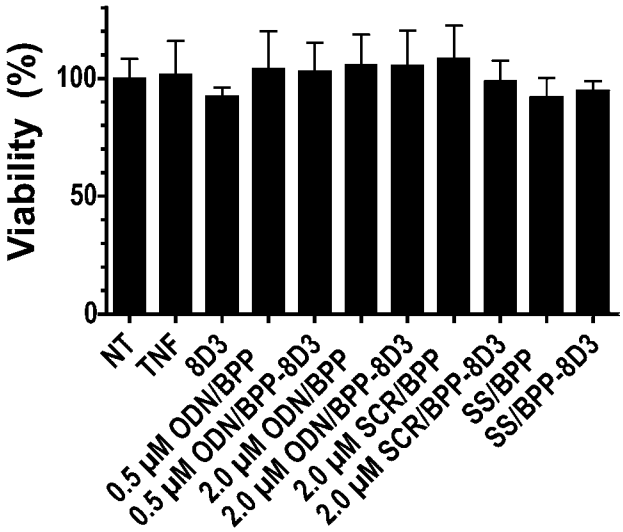

Fig. 2. Viability of bEnd5 cells measured by EZ4U assay under different treatment conditions and normalized to non-treated cells (NT) set to 100%. Samples were as follows: media control = TNFα only, ODN/BPP = complex of specific NF-κB decoy and BPP, SCR/BPP = complex of scrambled ODN and BPP, ODN/BPP-8D3 = specific complex with vector 8D3SA, 8D3 = 8D3SA vector only, SS/BPP = complex of salmon sperm DNA and BPP, SS/BPP-8D3 = salmon sperm DNA complex with vector 8D3SA, SCR/BPP-8D3 = scrambled ODN complex with vector 8D3SA. Molar concentrations refer to ODN; salmon sperm DNA was used at a weight concentration of 10 μg/ml DNA; 8D3SA concentrations were 0.083 μM. Values are shown as mean±SD, n=6.

cytotoxic effect of ODN/BPP complexes with the vector 8D3SA was also assessed. As shown in Fig. 2, the viability of the bEnd5 cells as determined with the MTT assay was unaltered under all treatment conditions compared to non-treated cells and to cells, which had only been stimulated with 50 ng/ml TNFα for 4 h (one way ANOVA, p>0.05).

Cellular Uptake of ODN/BPP Complexes

Figure 3 depicts bEnd5 cells incubated for 2 h with the fluorescent labeled ODN/BPP complexes with or without the targeting vector 8D3SA. At that time point, targeting to the transferrin receptor resulted in the detection of multiple complexes at unambiguously intracellular location (panels A–C). In contrast, ODN/BPP complexes without the 8D3SA vector formed larger aggregates on the cell surface, with little evidence of internalization (panels E–G). In both cases the confocal scans provided evidence of co-localization of FITC-labeled ODN and rhodamine-labeled PEI, indicating the integrity of the ODN/PEI complexes.

Effect of ODN/BPP on Gene Expression of Adhesion Molecules

To determine specific pharmacological effects of the decoy ODN, we quantitatively measured mRNA expression of adhesion molecules VCAM-1 (both full length and truncated), ICAM-1, inducible nitric oxide synthase (iNOS), and the inhibitor component of NF-κB complexes, IκBα, by RT-PCR. As shown in Fig. 4A, stimulation of bEnd5 cells with TNFα leads to an upregulation of full length VCAM-1 mRNA by a factor of 169 compared to naïve cells. The truncated mRNA for the GPI-anchored VCAM-1 splice variant was 47-fold increased (Fig. 4B). Treatment of bEnd5 cells with ODN/BPP complexes containing NF-κB decoys significantly inhibited upregulation of VCAM-1 mRNA by TNFα: With targeted cellular uptake using the 8D3SA vector, NF-κB decoy at a 0.5 μM concentration resulted in significantly lower mRNA levels. Compared to media controls, mRNA expression was lower by factors of 16.2 (full length VCAM-1, Fig. 4A) and 6.4 (truncated VCAM-1, Fig. 4B). Moreover, the presence of serum did not appreciably change the potent pharmacologic effect of 8D3SA targeted ODN/BPP complexes (Fig. 4C). In contrast, complexes without 8D3SA could not significantly affect VCAM-1 mRNA levels even at 2 μM concentration of decoy ODN, if serum was present (Fig. 4C). Without serum, there was a modest effect at higher NF-κB decoy concentrations of 1 and 2 μM (Fig. 4A, B).

To exclude non-specific effects of DNA/BPP complexes on VCAM-1 gene expression, we also quantified VCAM-1 mRNA in cells treated with complexes of BPP and salmon sperm DNA, with or without targeting by 8D3SA. No effect on mRNA expression levels after stimulation with TNFα was observed with this non-specific DNA. As would be expected from a NF-κB decoy, the inhibitory action of ODN/BPP complexes could also be demonstrated for other gene products, which the transcription factor regulates. Figure 5 shows the effects on mRNA expression in bEnd5 cells for ICAM-1, iNOS and the inhibitor IκBα. TNFα treatment stimulated the mRNA level 5.3-fold (IκBα), 23-fold (ICAM-1) and 137-fold (iNOS). In all three cases ODN/BPP complexes with NF-κB decoy inhibited the mRNA upregulation. The effect was strongest for complexes coupled to 8D3SA. The vector alone, or complex containing non-specific DNA (salmon sperm DNA) with or without vector, was ineffective.

As an additional control for the specificity of pharmacological effects, we quantified the mRNA levels of the constitutively expressed GAPDH gene product, which is not under regulatory influence by NF-κB. As shown in Fig. 6, there was no significant change under any of the treatment conditions applied to the bEnd5 cells.

In order to expand the quantitative evaluation of pharmacological effect, we then assessed separately the concentration response for the targeting vector 8D3SA and the decoy ODN. First, a constant concentration of ODN/BPP equivalent to 0.5 μM ODN was used. As can be inferred from Fig. 7A, 8D3SA concentrations as low as 0.083 μM were sufficient to mediate cellular uptake of the complexes and significantly inhibit VCAM-1 mRNA upregulation compared to controls. On the other hand, when ODN/BPP concentrations were varied while 8D3SA was held constant at 0.083 μM, NF-κB decoy ODN at concentrations as low as 0.05 μM still significantly inhibited VCAM-1 upregulation by TNFα (Fig. 7B).

We measured the adhesion of monocytes to a bEnd5 monolayer to answer the question whether inhibition of NF-κB mediated gene expression at the mRNA level translates into effects on endothelial cell function. As shown in Fig. 8, treatment of bEnd5 cells with ODN/BPP significantly decreased adhesion of fluorescently labeled U-937 cells to the endothelial cells. The complexes targeted to the transfer-

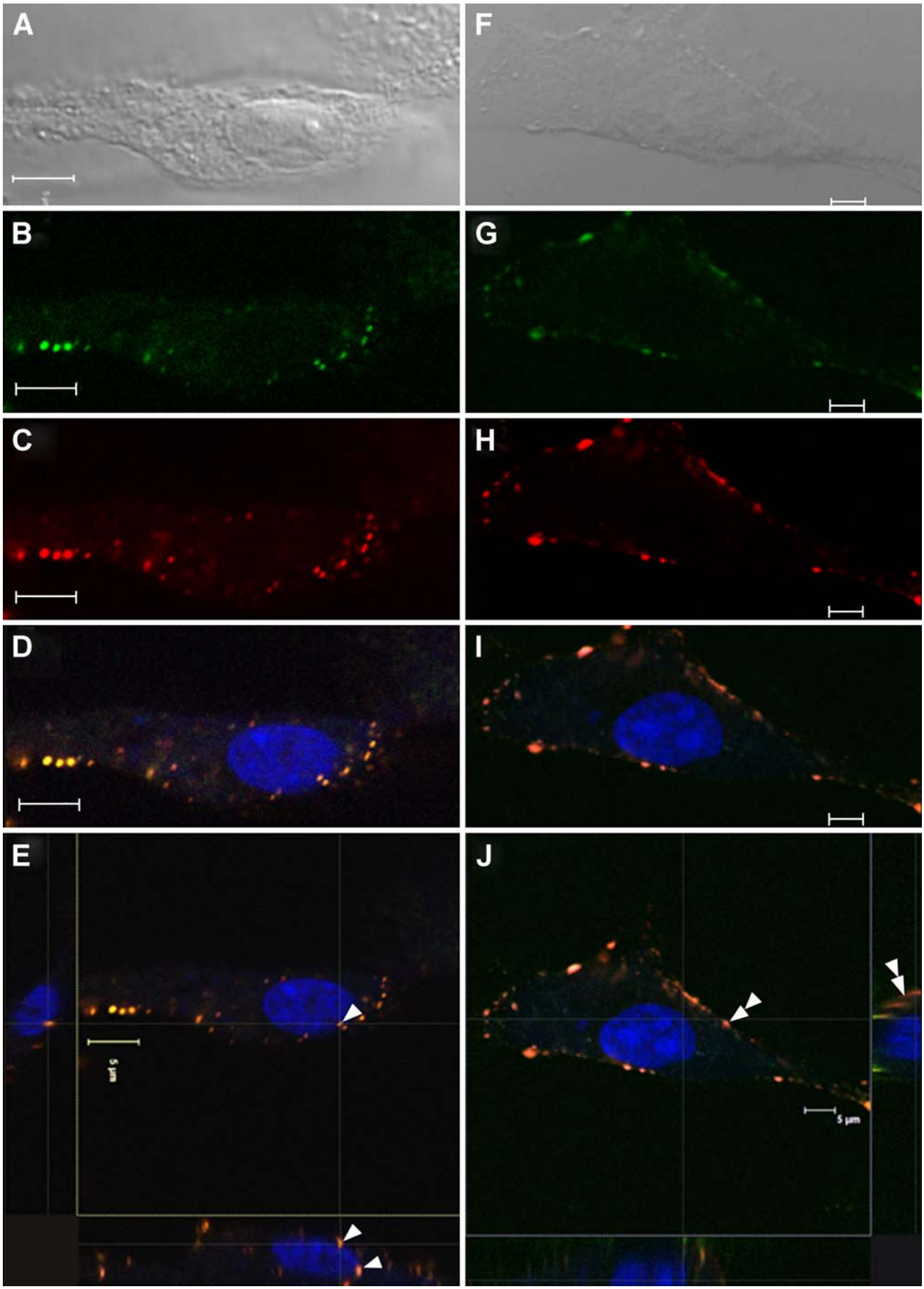
A
F
B
G
C
H
D
I
E
J
5 µm

Fig. 3. Confocal microscopy of bEnd5 cells after 2 h incubation with double-labeled ODN/BPP complexes with 8D3SA (**A**–**E**) or without 8D3SA (**F**–**J**). Subpanels **A** and **F** show DIC of the cells in subpanels (**B**–**E**) and (**G**–**J**), respectively. FITC-labeled ODN was visualized by excitation at 488 nm and emission bandwidth 500–535 nm (**B**, **G**); rhodamine-labeled BPP was visualized by excitation at 546 nm and emission bandwidth 560–600 (**C**, **H**); nuclear staining with DRAQ5 was visualized by excitation at 633 nm and emission bandwidth 650–700 nm (**D**, **E**, **I**, **J**). Subpanels **D** and **I** show the merged channels of subpanels **A**, **B** and **E**, **F** plus the nuclear stain. **B**–**D** and **G**–**I** represent single optical sections, while **E** and **J** represent Z-stacks of the corresponding cells. The arrowheads in subpanel **E** indicate internalized complexes in perinuclear localization. Double arrowheads in subpanel **J** indicate complexes associated with the cell membrane. Scale bars=5 μm.

rin receptor were only effective when they contained specific NF-κB decoy ODN (0.5 μM). No effect occurred, even at higher concentration, after treatment with complexes containing a scrambled version of the ODN or salmon sperm DNA. Moreover, this functional assay gave a virtually identical result when performed in the absence (Fig. 8A) or presence (Fig. 8B) of serum.

DISCUSSION

The present studies demonstrate potent pharmacological effects of NF-κB decoys on brain-derived endothelial cells following receptor-mediated delivery of ODN/BPP polyplexes. These targeted polyplexes consisted of biotinylated PEG-PEI and a 20mer double-stranded phosphodiester ODN. Quantitative measurements of NF-κB dependent gene transcripts by RT-PCR confirmed the specificity of the effect at the molecular level.

With the ultimate goal being drug activity following systemic administration, any nanoparticle- or polyplex-based delivery system has to meet several prerequisites. The first criterion is adequate stability in physiological fluids. The complexes of BPP and ODN used here were stable for at least 1 week at physiological salt concentration and pH, as well as in the presence of serum proteins (Fig. 1). The physicochemical stability is due to the PEG moiety of the co-polymer. DNA/PEI complexes formed with non-PEGylated 2.7 kDa PEI had previously shown rapid aggregation at physiological salt concentrations to sizes >500 nm within 10 min (20). Such a

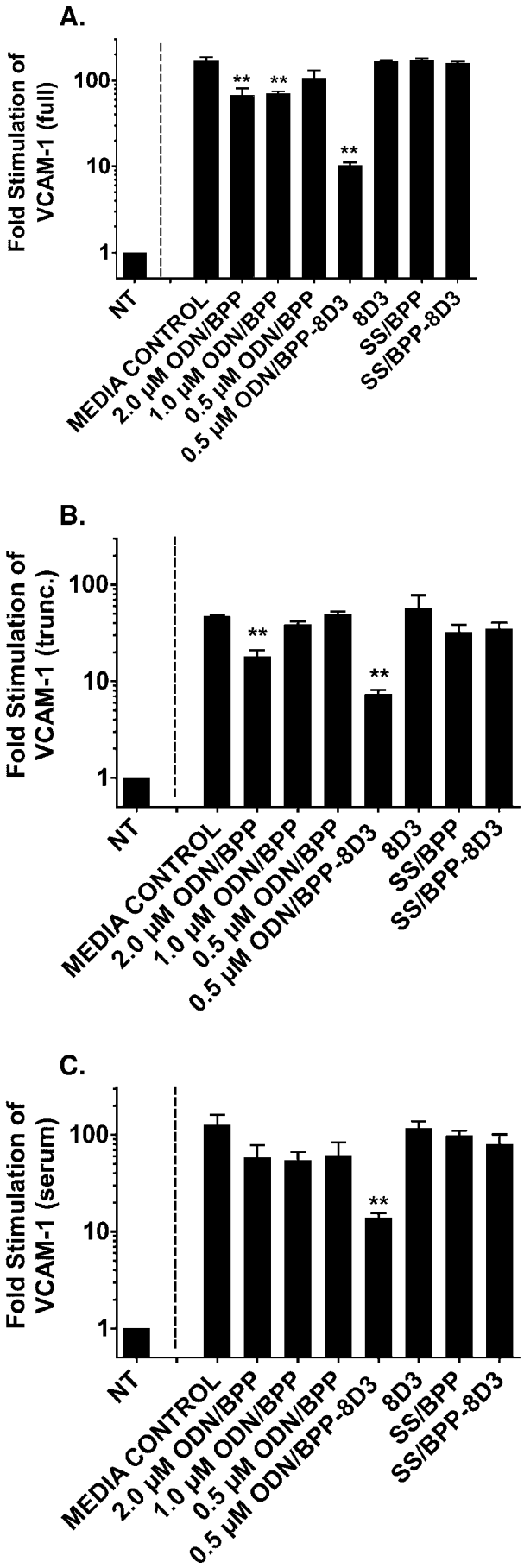

Fig. 4. mRNA expression of bEnd5 cells for VCAM-1 full-length isoform (**A**, **C**) and truncated isoform (**B**) as measured by RT-PCR. Values are shown as mean±SE, n=3. Treatment conditions were as follows: NT = non-treated, media control = TNFα only (4 h), ODN/BPP = complex of specific NF-κB decoy and BPP, ODN/BPP-8D3 = specific complex with vector 8D3SA, 8D3 = 8D3SA vector only, SS/BPP = complex of salmon sperm DNA and BPP, SS/BPP-8D3 = salmon sperm DNA complex with vector 8D3SA. Molar concentrations refer to ODN; salmon sperm DNA was used at a weight concentration of 10 μg/ml DNA; 8D3SA concentrations were 0.75 μM. Treatment with complexes was performed in serum free media (**A**, **B**) or in the presence of 10% FCS (**C**). VCAM-1 signal was normalized to 18S RNA and expressed as fold stimulation relative to NT=1. Notice the log-scale for the effect. $^{**}p<0.01$ vs. media control (ANOVA with Dunnett's multiple comparison test).

propensity to form large aggregates at physiological salt concentrations is known for other forms of PEI, like the high molecular weight 800 kDa PEI (21) and the linear 22 kDa PEI (22,23), which is more closely related to the low molecular weight, low-branched type of PEI used here (14).

Another criterion to consider for nano-particulate delivery systems is the mechanism of cellular uptake. Confocal fluorescence microscopy studies revealed that polyplexes made of PEI and DNA or RNA enter cells by the endocytotic route (24,25). In the case of non-PEGylated PEI this uptake process is triggered by electrostatic interactions of DNA/polycation complexes and the negatively charged cell membrane. PEGylation attenuates nonspecific uptake and enables the redirection of such complexes to specific, receptor-mediated targets (26,27). Here we analyzed differences in the cellular uptake between non-targeted complexes (ODN/BPP without 8D3SA) and the targeted complexes (with 8D3SA). Double fluorescent labeling of complexes allowed to unambiguously detect intact ODN/BPP complexes by co-localization of rhodamine-labeled BPP and FITC-labeled ODN. The specific binding by 8D3 to transferrin receptors caused internalization of complexes over a 2 h incubation period and resulted in the labeling of multiple intracellular vesicles with a size and morphology compatible to endosomes or lysosomes (Fig. 3A–D). PEI is known to disrupt endosomes and release polymer and ODN into the cytosol and nucleus (24,25,28). In the present study a low concentration of complex was used to load the cells, which matched the conditions in the pharmacological experiments (equivalent to 2 μM ODN). Therefore, the resulting cytosolic or nuclear concentrations following release from endosomes were likely too low for optical observation.

In contrast to the targeted polyplexes, ODN/BPP without 8D3SA mostly decorated the cell membrane (Fig. 3E–H). The cell surface adhesion of non-targeted polyplexes results from residual adsorptive mechanisms, i.e. electrostatic interaction between negatively charged cell membrane and a positive surface charge of the ODN/BPP complexes. In agreement with this explanation, a weakly positive ζ-potential value of 13.7±5 mV was measured for polyplexes at the N/P ratio of 6:1 and pH 7.4.

At a functional level, the current results expand our previous data, which demonstrated the suitability of PEI to transfect endothelial cells with transcription factor decoys, downregulate NF-κB dependent gene expression in endothelial cells, and inhibit monocyte adhesion (2). Notably, ODN/BPP polyplexes targeted to transferrin receptors by the 8D3 antibody significantly increased the pharmacological potency of the NF-κB decoy, in either the absence or presence of serum proteins.

While PEGylated, ligand-coupled PEIs targeting cell surface receptors have been broadly explored as vectors for nonviral delivery of genes (27,29–31), antisense oligonucleotides (32,33) and siRNA (34,35), the cellular delivery of transcription factor decoys with such a construct has not been reported to our knowledge. Among the multiple forms of PEGylated PEIs described in recent years, the PEI-derivative used here is most closely related to a PEGylated PEI synthesized by Kabanov's group (32,33). These investigators delivered a 20-mer antisense PS-ODN using a copolymer, which consisted of two strands of 8 kDa PEG (either with or

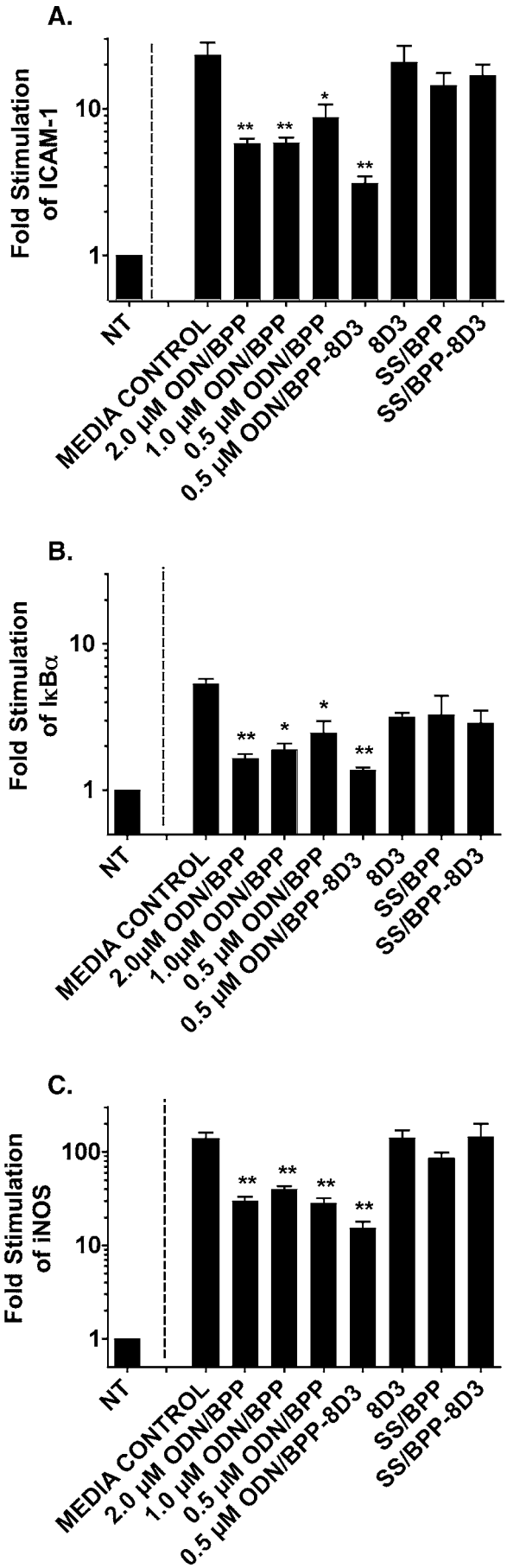

Fig. 5. mRNA expression of bEnd5 cells for ICAM-1 (**A**) IκBα (**B**) and iNOS (**C**) as measured by RT-PCR. Values are shown as mean±SE, n=3. Treatment conditions were as follows: NT = non-treated, media control = TNFα only (4 h), ODN/BPP = complex of specific NF-κB decoy and BPP, ODN/BPP-8D3 = specific complex with vector 8D3SA, 8D3 = 8D3SA vector only, SS/BPP = complex of salmon sperm DNA and BPP, SS/BPP-8D3 = salmon sperm DNA complex with vector 8D3SA. Molar concentrations refer to ODN; salmon sperm DNA was used at a concentration of 10 ug/ml DNA; 8D3SA concentrations were 0.75 μM. ICAM-1, IκBα and iNOS signals were normalized to 18S RNA and expressed as fold stimulation relative to NT=1. Notice the log-scale for the effect. *p<0.05, **p<0.01 vs. media control (ANOVA with Dunnett's multiple comparison test).

without terminal biotin) grafted to commercial 2 kDa PEI (33). Their copolymer/ODN complexes were then coupled to the targeting ligand, biotinylated transferrin, in a 2-step approach via an avidin bridge, resulting in particle sizes of about 100 nm. Concordant with that paper, the data obtained here with complexes of 20mer double-stranded ODN and a 1:1 copolymer of 2.7 kDa PEI and 3.7 kDa biotin-PEG are further proof that low molecular weight PEIs tolerate high degrees of PEGylation. Such PEG-PEIs do not loose the ability to tightly bind oligonucleotides in complexes, which are both stable towards physiological fluids including serum, and efficient as cellular transfection vehicles.

At a concentration of up to 2 μM of decoy ODN in presence of serum, the non-targeted complexes were ineffective in attenuating the TNFα-stimulated increase in VCAM-1 gene expression, while as little as 0.05 μM decoy ODN potently inhibited the increase in mRNA levels (Figs. 4C and 7B). In this context, it is noteworthy that the ODN used in the present study was an unmodified phosphodiester ODN. Regardless of the delivery systems used, most work with transcription factor decoys employed metabolically stabilized ODNs, e.g. phosphorothioate derivatives (PS-ODN) (36–38). PS-ODNs in particular have been shown to be prone to sequence independent cellular effects (39). Taking advantage of the protective action of PEI against enzymatic degradation, unmodified ODN could be applied here. To rule out nonspecific effects on gene transcription by ODN/BPP

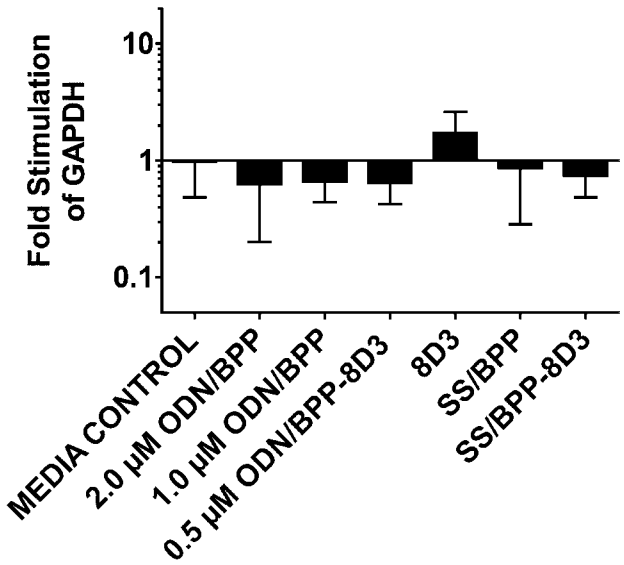

Fig. 6. mRNA expression of bEnd5 cells for the housekeeping gene GAPDH as measured by RT-PCR. Expression levels were standardized with 18s RNA. The GAPDH signal in cells without any treatment was set to 1. Values are shown as mean±SE, n=3. Notice the different range of log-scale compared to Fig. 5. Treatment conditions were as follows: NT = non-treated, media control = TNFα only (4 h), ODN/BPP = complex of specific NF-κB decoy and BPP, ODN/BPP-8D3 = specific complex with vector 8D3SA, 8D3 = 8D3SA vector only, SS/BPP = complex of salmon sperm DNA and BPP, SS/BPP-8D3 = salmon sperm DNA complex with vector 8D3SA. Molar concentrations refer to ODN. Salmon sperm DNA was used at a weight concentration of DNA equivalent to 2 μM ODN. 8D3SA concentrations were 0.75 μM. p>0.05 (ANOVA).

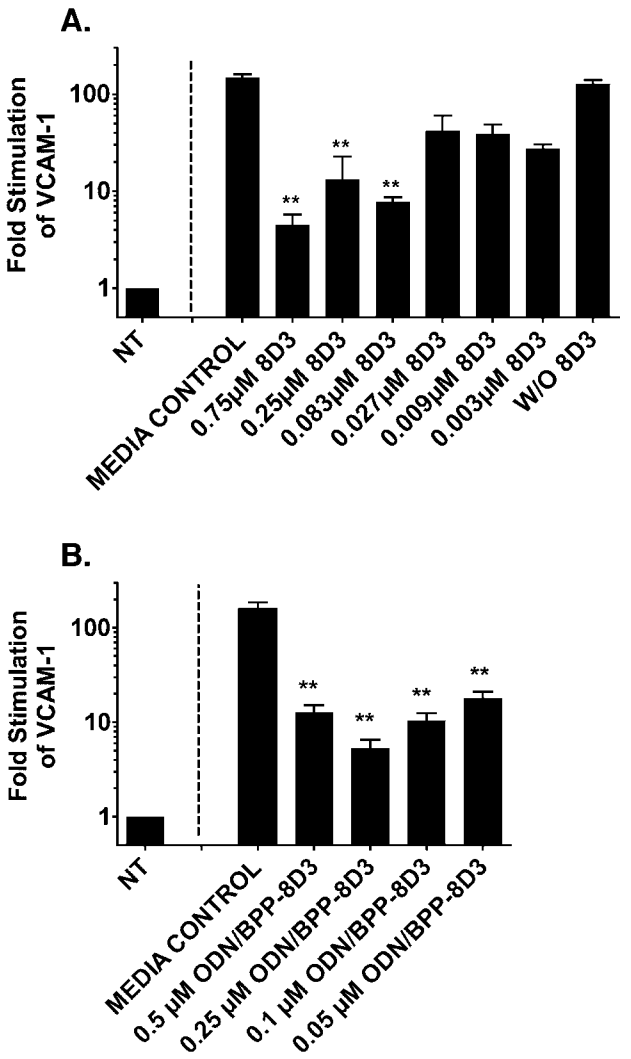

Fig. 7. **A** Efficacy of different concentrations of the 8D3SA vector attached to ODN/BPP complexes (all 0.5 μM) to inhibit the expression of VCAM-1 mRNA under stimulation by TNFα. **B** Efficacy of different concentrations of ODN/BPP complexes (concentrations refer to ODN) targeted by the vector 8D3SA (all 0.083 μM) to inhibit the expression of VCAM-1 mRNA under stimulation by TNFα. Values are shown as mean±SE, n=3. VCAM-1 signal was normalized to 18S RNA and expressed as fold stimulation relative to NT=1. Notice the log-scale for the effect in (**A**) and (**B**). **p<0.01 vs. media control (ANOVA with Dunnett's multiple comparison test).

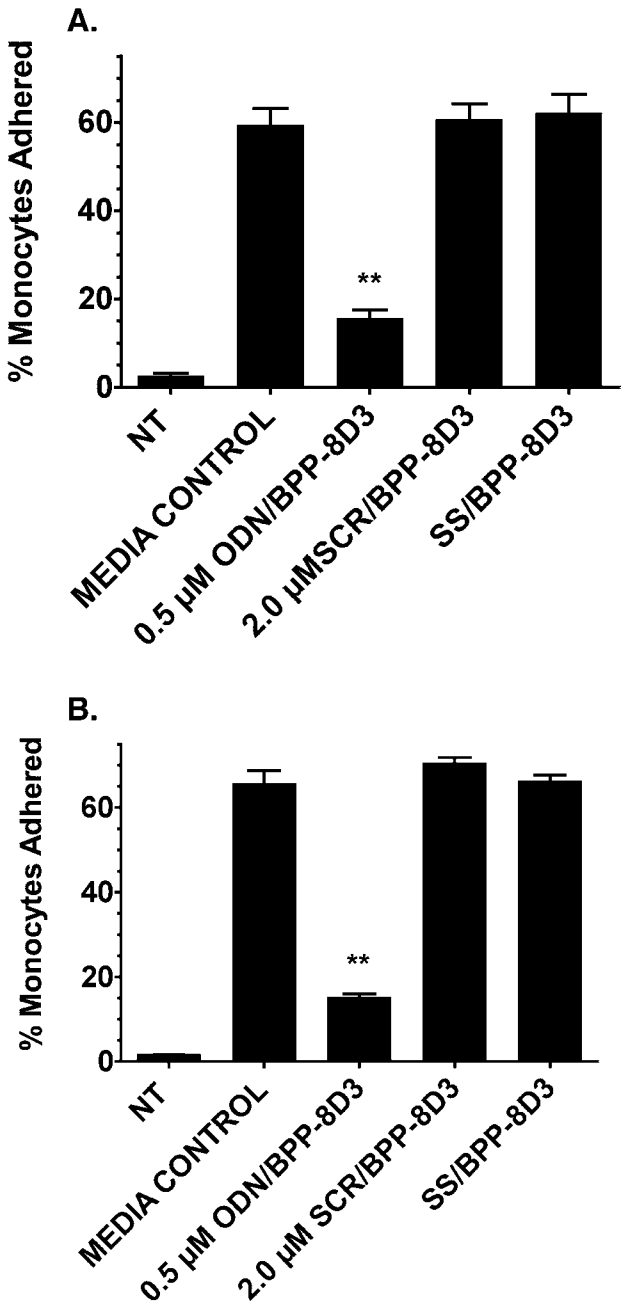

Fig. 8. Adhesion of fluorescently labeled U937 monocytes to bEnd5 monolayers after stimulation of the endothelial cells with TNF**α**. Treatment conditions were as follows in serum free media (**A**), or in the presence of 10% FCS (**B**) NT = non-treated, media control = TNFα only, 0.5 μM ODN/BPP-8D3 = bEnd5 cells treated with the specific complex and targeted with 8D3SA, 2 μM SCR/BPP-8D3 = bEnd5 cells treated with complexes containing scrambled ODN and targeted with 8D3SA, SS/BPP-8D3 = bEnd5 cells treated with complexes containing salmon sperm DNA. $^{**}p<0.01$ vs. media control (ANOVA with Dunnett's multiple comparison test).

polyplexes, the mRNA expression of a house keeping gene, GAPDH, was also quantified and standardized to cellular 18S RNA. No significant changes were found under any of the treatment conditions.

Finally, the downstream functional effect of inhibiting NF-κB dependent transcription of adhesion molecules resulted in profoundly decreased monocyte adhesion to TNFα stimulated bEnd5 endothelial cells. This corresponds to results seen after treatment of endothelial cells with non-derivatized PEI (2) and is likely due to the simultaneous inhibition of several adhesion molecules, in particular VCAM-1 and ICAM-1. In the previous report only the presence of both VCAM-1 and ICAM-1 blocking antibodies achieved a comparable level of inhibition of monocyte adhesion.

CONCLUSIONS

The present approach represents a promising option to fight inflammatory responses at the BBB. The pharmacological effects obtained with non-targeted polyplexes for cellular delivery of NF-κB decoys were retained in the current biotinylated and PEGylated derivative of low molecular weight PEI, which allows facile coupling to targeting antibodies via (strept)avidin linkage. While NF-κB decoys consisting of native phosphodiester ODNs showed potent effects at the mRNA level and at the functional level (cell adhesion) when delivered by 8D3-targeted polyplexes, activity of polyplexes without the transferrin receptor antibody was markedly reduced or absent. Moreover, polyplexes carrying control DNA had no measurable effects. Compared to ubiquitous blockade of integrins on all lymphocytes, as realized in the case of α4-integrin antibodies, the selective inhibition of adhesion molecules in a disease-relevant vascular bed, e.g. in brain microvasculature, may cause less immunosuppression and should be less prone to adverse effects (40). To substantiate this hypothesis, *in vivo* studies in models of neuroinflammation are currently pursued. *In vivo* efficacy will depend (i) on stability of the complexes in blood, and (ii) on their pharmacokinetics and organ distribution due to transferrin receptor-targeting. With respect to stability, the results obtained here indicate good physical integrity in the presence of serum proteins. In addition, the protection against DNAse degradation of native double stranded phosphodiester ODN, as used here, by PEI complexation has previously been shown (6). Therefore, the utilization of stabilized ODN, like phosphorothioate derivatives, should not be required in the *in vivo* setting.

ACKNOWLEDGMENTS

The authors thank Dr. Holger Petersen (Basel) for synthesis and analysis of the biotin-PEG-PEI copolymer and Young Tag Ko for preparation of the rhodamine-biotin-PEG-PEI conjugate. We appreciate the helpful discussions with Dr. Thomas Kissel (Marburg). This work was supported by grant 1R01NS045043 to UB.

REFERENCES

1. M. J. Mann. Transcription factor decoys: a new model for disease intervention. *Ann. N. Y. Acad. Sci.* **1058**:128–139 (2005).
2. D. Fischer, R. Bhattacharya, B. Osburg, and U. Bickel. Inhibition of monocyte adhesion on brain-derived endothelial

cells by NF-kappaB decoy/polyethylenimine complexes. *J. Gene Med.* **7**:1063–1076 (2005).
3. L. Steinman. Blocking adhesion molecules as therapy for multiple sclerosis: natalizumab. *Nat. Rev., Drug Discov.* **4**:510–518 (2005).
4. T. A. Yednock, C. Cannon, L. C. Fritz, F. Sanchez-Madrid, L. Steinman, and N. Karin. Prevention of experimental autoimmune encephalomyelitis by antibodies against alpha 4 beta 1 integrin. *Nature* **356**:63–66 (1992).
5. D. H. Miller, O. A. Khan, W. A. Sheremata, L. D. Blumhardt, G. P. Rice, M. A. Libonati, A. J. Willmer-Hulme, C. M. Dalton, K. A. Miszkiel, and P. W. O'Connor. A controlled trial of natalizumab for relapsing multiple sclerosis. *N. Engl. J. Med.* **348**:15–23 (2003).
6. D. Fischer, B. Osburg, H. Petersen, T. Kissel, and U. Bickel. Effect of poly(ethylene imine) molecular weight and pegylation on organ distribution and pharmacokinetics of polyplexes with oligodeoxynucleotides in mice. *Drug Metab. Dispos.* **32**:983–992 (2004).
7. U. Bickel, T. Yoshikawa, and W. M. Pardridge. Delivery of peptides and proteins through the blood–brain barrier. *Adv. Drug Deliv. Rev.* **46**:247–279 (2001).
8. W. M. Pardridge. Blood–brain barrier drug targeting: the future of brain drug development. *Mol. Interv.* **3**:90–105 (2003).
9. H. J. Lee, B. Engelhardt, J. Lesley, U. Bickel, and W. M. Pardridge. Targeting rat anti-mouse transferrin receptor monoclonal antibodies through blood–brain barrier in mouse. *J. Pharmacol. Exp. Ther.* **292**:1048–1052 (2000).
10. H. J. Lee, Y. Zhang, C. Zhu, K. Duff, and W. M. Pardridge. Imaging brain amyloid of Alzheimer disease *in vivo* in transgenic mice with an Abeta peptide radiopharmaceutical. *J. Cereb. Blood Flow Metab.* **22**:223–231 (2002).
11. N. Shi, Y. Zhang, C. Zhu, R. J. Boado, and W. M. Pardridge. Brain-specific expression of an exogenous gene after i.v. administration. *Proc. Natl. Acad. Sci. U. S. A.* **98**:12754–12759 (2001).
12. Y. Zhang and W. M. Pardridge. Delivery of beta-galactosidase to mouse brain via the blood–brain barrier transferrin receptor. *J. Pharmacol. Exp. Ther.* **313**:1075–1081 (2005).
13. H. J. Lee, R. J. Boado, D. A. Braasch, D. R. Corey, and W. M. Pardridge. Imaging gene expression in the brain *in vivo* in a transgenic mouse model of Huntington's disease with an antisense radiopharmaceutical and drug-targeting technology. *J. Nucl. Med.* **43**:948–956 (2002).
14. D. Fischer, T. Bieber, Y. Li, H. P. Elsasser, and T. Kissel. A novel non-viral vector for DNA delivery based on low molecular weight, branched polyethylenimine: effect of molecular weight on transfection efficiency and cytotoxicity. *Pharm. Res.* **16**:1273–1279 (1999).
15. M. Laschinger and B. Engelhardt. Interaction of alpha4-integrin with VCAM-1 is involved in adhesion of encephalitogenic T cell blasts to brain endothelium but not in their transendothelial migration *in vitro*. *J. Neuroimmunol.* **102**:32–43 (2000).
16. A. von Harpe, H. Petersen, Y. Li, and T. Kissel. Characterization of commercially available and synthesized polyethylenimines for gene delivery. *J. Control. Release* **69**:309–322 (2000).
17. B. Osburg. *Drug delivery of Oligonucleotides at the Blood–Brain Barrier: A Therapeutic Strategy for Inflammatory Diseases of the Central Nervous System, Physiology*, Philipps-University, Marburg, 2003.
18. M. I. Cybulsky, M. Allan-Motamed, and T. Collins. Structure of the murine VCAM1 gene. *Genomics* **18**:387–391 (1993).
19. R. K. Rohnelt, G. Hoch, Y. Reiss, and B. Engelhardt. Immunosurveillance modelled *in vitro*: naive and memory T cells spontaneously migrate across unstimulated microvascular endothelium. *Int. Immunol.* **9**:435–450 (1997).
20. K. Kunath, A. Harpevon, D. Fischer, H. Petersen, U. Bickel, K. Voigt, and T. Kissel. Low-molecular-weight polyethylenimine as a non-viral vector for DNA delivery: comparison of physicochemical properties, transfection efficiency and *in vivo* distribution with high-molecular-weight polyethylenimine. *J. Control. Release* **89**:113–125 (2003).
21. M. Ogris, P. Steinlein, M. Kursa, K. Mechtler, R. Kircheis, and E. Wagner. The size of DNA/transferrin-PEI complexes is an important factor for gene expression in cultured cells. *Gene Ther.* **5**:1425–1433 (1998).
22. D. Goula, J. S. Remy, P. Erbacher, M. Wasowicz, G. Levi, B. Abdallah, and B. A. Demeneix. Size, diffusibility and transfection performance of linear PEI/DNA complexes in the mouse central nervous system. *Gene Ther.* **5**:712–717 (1998).
23. L. Wightman, R. Kircheis, V. Rossler, S. Carotta, R. Ruzicka, M. Kursa, and E. Wagner. Different behavior of branched and linear polyethylenimine for gene delivery *in vitro* and *in vivo*. *J. Gene Med.* **3**:362–372 (2001).
24. W. T. Godbey, K. K. Wu, and A. G. Mikos. Tracking the intracellular path of poly(ethylenimine)/DNA complexes for gene delivery. *Proc. Natl. Acad. Sci. U. S. A.* **96**:5177–5181 (1999).
25. T. Merdan, K. Kunath, D. Fischer, J. Kopecek, and T. Kissel. Intracellular processing of poly(ethylene imine)/ribozyme complexes can be observed in living cells by using confocal laser scanning microscopy and inhibitor experiments. *Pharm. Res.* **19**:140–146 (2002).
26. T. Merdan, J. Kopecek, and T. Kissel. Prospects for cationic polymers in gene and oligonucleotide therapy against cancer. *Adv. Drug Deliv. Rev.* **54**:715–758 (2002).
27. R. Kircheis, L. Wightman, and E. Wagner. Design and gene delivery activity of modified polyethylenimines. *Adv. Drug Deliv. Rev.* **53**:341–358 (2001).
28. O. Boussif, F. Lezoualc'h, M. A. Zanta, M. D. Mergny, D. Scherman, B. Demeneix, and J. P. Behr. A versatile vector for gene and oligonucleotide transfer into cells in culture and *in vivo*: polyethylenimine. *Proc. Natl. Acad. Sci. U. S. A.* **92**:7297–7301 (1995).
29. M. Ogris, P. Steinlein, S. Carotta, S. Brunner, and E. Wagner. DNA/polyethylenimine transfection particles: influence of ligands, polymer size, and PEGylation on internalization and gene expression. *AAPS PharmSci.* **3**:E21 (2001).
30. O. Germershaus, T. Merdan, U. Bakowsky, M. Behe, and T. Kissel. Trastuzumab-polyethylenimine-polyethylene glycol conjugates for targeting her2-expressing tumors. *Bioconjug. Chem.* **17**:1190–1199 (2006).
31. A. Kichler. Gene transfer with modified polyethylenimines. *J. Gene Med.* **6**(Suppl 1):S3–S10 (2004).
32. S. V. Vinogradov, T. K. Bronich, and A. V. Kabanov. Self-assembly of polyamine-poly(ethylene glycol) copolymers with phosphorothioate oligonucleotides. *Bioconjug. Chem.* **9**:805–812 (1998).
33. S. Vinogradov, E. Batrakova, S. Li, and A. Kabanov. Polyion complex micelles with protein-modified corona for receptor-mediated delivery of oligonucleotides into cells. *Bioconjug. Chem.* **10**:851–860 (1999).
34. R. M. Schiffelers, A. Ansari, J. Xu, Q. Zhou, Q. Tang, G. Storm, G. Molema, P. Y. Lu, P. V. Scaria, and M. C. Woodle. Cancer siRNA therapy by tumor selective delivery with ligand-targeted sterically stabilized nanoparticle. *Nucleic Acids Res.* **32**:e149 (2004).
35. S. Mao, M. Neu, O. Germershaus, O. Merkel, J. Sitterberg, U. Bakowsky, and T. Kissel. Influence of polyethylene glycol chain length on the physicochemical and biological properties of poly(ethylene imine)-graft-poly(ethylene glycol) block copolymer/SiRNA polyplexes. *Bioconjug. Chem.* **17**:1209–1218 (2006).
36. R. Morishita, T. Sugimoto, M. Aoki, I. Kida, N. Tomita, A. Moriguchi, K. Maeda, Y. Sawa, Y. Kaneda, J. Higaki, and T. Ogihara. *In vivo* transfection of cis element "decoy" against nuclear factor-kappaB binding site prevents myocardial infarction. *Nat. Med.* **3**:894–899 (1997).
37. S. Fichtner-Feigl, I. J. Fuss, J. C. Preiss, W. Strober, and A. Kitani. Treatment of murine Th1- and Th2-mediated inflammatory bowel disease with NF-kappa B decoy oligonucleotides. *J. Clin. Invest.* **115**:3057–3071 (2005).
38. C. Desmet, P. Gosset, B. Pajak, D. Cataldo, M. Bentires-Alj, P. Lekeux, and F. Bureau. Selective blockade of NF-kappa B activity in airway immune cells inhibits the effector phase of experimental asthma. *J. Immunol.* **173**:5766–5775 (2004).
39. J. R. Perez, Y. Li, C. A. Stein, S. Majumder, A. Oorschotvan, and R. Narayanan. Sequence-independent induction of Sp1 transcription factor activity by phosphorothioate oligodeoxynucleotides. *Proc. Natl. Acad. Sci. U. S. A.* **91**:5957–5961 (1994).
40. R. M. Ransohoff. Natalizumab and PML. *Nat. Neurosci.* **8**:1275 (2005).